Biogeosciences Discuss., 7, 7271–7314, 2010
www.biogeosciences-discuss.net/7/7271/2010/
doi:10.5194/bgd-7-7271-2010

Biogeosciences Discussions

Air-sea CO_2 fluxes on the Bering Sea shelf

N. R. Bates[1], **J. T. Mathis**[2], **and M. A. Jeffries**[3]

[1]Bermuda Institute of Ocean Sciences, Ferry Reach, Bermuda
[2]University of Alaska-Fairbanks, Fairbanks, USA
[3]University of Victoria, Victoria, Canada

Received: 13 September 2010 – Accepted: 17 September 2010 – Published: 5 October 2010

Correspondence to: N. R. Bates (nick.bates@bios.edu)

Published by Copernicus Publications on behalf of the European Geosciences Union.

Abstract

There have been few previous studies of surface seawater CO_2 partial pressure (pCO_2) variability and air-sea CO_2 gas exchange rates for the Bering Sea shelf which is the largest US coastal shelf sea. In 2008, spring and summertime observations were collected in the Bering Sea shelf as part of the Bering Sea Ecological Study (BEST). Our results indicate that the Bering Sea shelf was close to neutral in terms of CO_2 sink-source status in springtime due to relatively small air-sea CO_2 gradients (i.e., ΔpCO_2) and sea-ice cover. However, by summertime, very low seawater pCO_2 values were observed and much of the Bering Sea shelf became strongly undersaturated with respect to atmosphere CO_2 concentrations. Thus the Bering Sea shelf transitions seasonally from mostly neutral conditions to a strong oceanic sink for atmospheric CO_2 particularly in the *"green belt"* region of the Bering Sea. Ocean biological processes dominate the seasonal drawdown of seawater pCO_2 for large areas of the Bering Sea shelf, with the effect partly countered by seasonal warming. In small areas of the Bering Sea shelf south of the Pribilof Islands and in the SE Bering Sea, seasonal warming is the dominant influence on seawater pCO_2, shifting localized areas of the shelf from minor/neutral CO_2 sink status to neutral/minor CO_2 source status, in contrast to much of the Bering Sea shelf. We compute that the Bering Sea shelf CO_2 sink in 2008 was 157 Tg C yr^{-1} (Tg=10^{12} g C) and a stronger sink for CO_2 than previously demonstrated by other studies.

1 Introduction

The Bering Sea shelf is one of the most productive marine ecosystems in the global ocean. Physical processes and seasonal sea-ice advance and retreat in the Bering Sea play a major role in controlling water mass properties and shaping the character of pelagic and benthic ecosystems found on the shelf. On the extensive continental shelf (Fig. 1), seasonally high rates of pelagic phytoplankton primary production (PP)

BGD
7, 7271–7314, 2010

supports large populations of marine mammals and seabirds, and coastal fisheries of Alaska. On the outer shelf of the Bering Sea, a region of elevated phytoplankton biomass termed the "*green belt*" has been observed in spring and summer for many decades (Hansell et al., 1989; Springer et al., 1996; Okkonen et al., 2004; Mathis et al., 2010a). Extensive, but sporadic blooms of coccolithophores, which are $CaCO_3$-producing phytoplankton (class *Prymnesiophyceae*) have also been observed in the SE Bering Sea shelf (e.g., Stockwell et al., 2001; Broerse et al., 2003; Merico et al., 2004, 2006). In contrast to the shelf, the open ocean regions of the Bering Sea is much less productive and has been described as a high nutrient, low chlorophyll (HNLC) region (Banse and English, 1999).

Over the last few decades, many studies have been conducted on the physical and biological character of the Bering Sea, but there have been few studies of the marine carbon cycle, air-sea CO_2 exchange rates or the potential impact of ocean acidification on the chemistry of shelf waters and ecosystems of the Bering Sea. In the open-ocean region of the Bering Sea, observations of seawater pCO_2 (i.e., partial pressure of CO_2) and dissolved inorganic carbon (DIC) have been collected close to the Western Aleutian Islands (e.g., Murphy et al., 2001; Nedashkovkii and Sapozhnikov, 2001; Wong et al., 2002) or outside the Bering Sea in the subarctic gyre of the North Pacific Ocean (e.g., Midorikawa et al., 2002; Murata and Takazawa, 2002). On the Bering Sea shelf, a few studies have shown that high summertime levels of phytoplankton primary production observed in the "*green belt*" result in a drawdown of seawater inorganic nutrients and DIC (and pCO_2) (e.g., Kelley and Hood, 1971; Park et al., 1974; Codispoti et al., 1982, 1986; Chen and Gao, 2007; Mathis et al., 2010a). Extensive coccolithophore blooms on the SE Bering Sea shelf should also seasonally decrease total alkalinity (TA) and DIC of seawater (as observed in other coastal seas and oceans; e.g., Robertson et al., 1994; Bates et al., 1996a), but at present, there has only been model assessments of the impact of coccolithophores on the ocean carbon cycle of the Bering Sea (Merico et al., 2004, 2006). Unlike other taxonomic classes of phytoplankton blooms, coccolithophores can increase seawater pCO_2 content and thus contribute

BGD
7, 7271–7314, 2010

to a negative coccolithophore-CO_2 feedback (Riebesall et al., 2000; Zondervan et al., 2001; Ridgewell et al., 2007) that has potentially important implications for the role of the global ocean in the uptake of anthropogenic CO_2, modulation of atmospheric CO_2 and climate responses over the next few centuries.

The contribution of the Bering Sea to the global ocean uptake of CO_2 is also highly uncertain. Early studies based on observations (Codispoti et al., 1982, 1986) and models (Walsh and Dieterle, 1994; Walsh et al., 1996) suggested that the entire Bering Sea was a potential sink for atmospheric CO_2. More recently, it has been reported that the Bering Sea acts as a net annual oceanic sink of CO_2 on the order of 200 Tg C yr^{-1} (Tg=10^{12} g C; Chen et al., 2004) and thus a significant contributor (>10%) to the annual global uptake of CO_2 (~1.4 Pg yr^{-1}; Takahashi et al., 2009). However, the seawater pCO_2 datasets of Takahashi et al. (2002; 2009) suggest that the open-ocean Bering Sea exhibits seasonal changes from a CO_2 sink in springtime (due to phytoplankton production) to a CO_2 source to the atmosphere in summertime (Takahashi et al., 2002). But, important caveats to note are that the seawater pCO_2 climatology has a coarse spatial resolution of 4°×5° and data was primarily collected from a relatively small open-ocean region of the Bering Sea (just north of the Aleutian Islands). Indeed, in the recent Takahashi et al. (2009) seawater pCO_2 climatology, only one cruise dataset across the Bering Sea shelf was deemed of sufficient quality to be included in the climatology.

Given the above uncertainties about the contribution of the Bering Sea shelf to the global ocean uptake of CO_2, it is important to improve assessments of the rate of air-sea CO_2 exchange for this coastal sea. In this paper, we examine the seasonal variability of inorganic carbon for the Bering Sea shelf observed in 2008 and determine the magnitude and timing of ocean CO_2 sinks and sources. We compare our observations with average conditions using the seawater pCO_2 climatology of Takahashi et al. (2009) and a seawater pCO_2 climatology based on a multiple-linear regression (MLR) model. Such assessment also serve as a baseline for understanding the potential changes in ocean CO_2 sinks and sources in responses to changes in physical forcing (e.g., circulation and mixing; nutrient supply; sea-ice advance/retreat timing and sea-ice extent;

BGD
7, 7271–7314, 2010

summer heating/winter cooling) and marine ecosystems (e.g., the rate, extent, timing and community structure of the spring phytoplankton bloom; presence/absence of cocolithophores, Stockwell et al., 2001). In complementary papers, the rate of net community production (NCP; Mathis et al., 2010a) and the impact of ocean acidification on the seawater carbonate chemistry of the Bering Sea shelf (Mathis et al., 2010b) have been reported.

2 Methods and materials

2.1 Physical and biological setting of the Bering Sea

The subpolar Bering Sea is a semi-enclosed basin (Fig. 1) with an extensive continental shelf in the east and deep open-ocean to the west. Physical processes and seasonal sea ice cover in the Bering Sea play a major role in controlling water mass properties and shaping the character of shelf pelagic and benthic ecosystems (e.g., McRoy and Goering, 1974; Wyllie-Echeverria and Ohtani, 1999; Stabeno et al., 2002; Grebmeier et al., 2006a, b). During the winter, sea-ice covers much of the Bering Sea shelf, but the advance is constrained by the presence of relatively warm water in the Central and Southern Bering Sea. During winter, water-masses are confined to a small range of temperature-salinity through vertical homogenization by ventilation, brine rejection and mixing. During the summertime, sea-ice retreats into the Chukchi Sea and Canada Basin of the Arctic Ocean. The extent of sea-ice cover and ecosystem structure undergoes significant interannual changes (e.g., Stabeno et al., 2001; Macklin et al., 2002; Hunt et al., 2002) that appear related to climatological changes in the Pacific Decadal Oscillation (PDO), Arctic Oscillation (AO) and El Niño-Southern Oscillation (ENSO), as well as long-term reduction in sea-ice extent (e.g., Springer, 1998; Hollowed et al., 2001; Hunt et al., 2002; Rho and Whitledge, 2007) that is linked to amplification of warming in the Arctic and sub-Arctic with subsequent reductions in sea-ice extent and thickness (e.g., Serreze et al., 2007).

BGD
7, 7271–7314, 2010

An extensive (>1000 km length) and broad (>500 km width) shelf, winter-time cross-shelf renewal of nutrients, vertical stability imposed by the flux of river runoff from the continent as well as by sea-ice formation and melt, and long hours of irradiance throughout the spring and summer, makes the Bering Sea shelf one of the most productive marine ecosystems in the world. This region supports millions of migratory marine birds relying on rich foraging during their breeding seasons, large populations of marine mammals restoring fat reserves lost over long winters of relative fasting, and commercially important fisheries (e.g., pollock and crab) that generate >50% of all fish and shellfish landings in the United States (Grebmeier et al., 2006a, b).

Over the past decade, the character of the marine ecosystem in the Bering Sea has exhibited considerable change (e.g., Stabeno et al., 2001; Macklin et al., 2002; Hunt et al., 2002; Bond et al., 2003; Bond and Overland, 2005; Grebmeier et al., 2006b, 2008). Cold-water, Arctic species have been replaced by organisms more indicative of temperate zones and reduced sea-ice cover has been proposed to favor a "phytoplankton–zooplankton" dominated ecosystem over the more typical "sea-ice algae–benthos" ecosystem indicative of Arctic Ocean shelves (including the Northern Bering Sea shelf) in particular (Piepenburg et al., 2005). Large, sweeping populations of jellyfish have come and gone (Napp et al., 2002), and coccolithophorid blooms that had become regular features of the SE Bering Sea (e.g., Stockwell et al., 2001; Broerse et al., 2003; Merico et al., 2004, 2006) have also been absent over the last few years. These lower trophic level changes cascade upward to impact higher trophic levels, evident in the decline in fur seal and sea lion populations that have coincided with large decreases in salmon runs to the rivers of Alaska. Further changes in physical forcings to the Bering Sea (Stabeno et al., 2001) will likely lead to further dramatic changes in the marine ecosystem, with uncertain feedbacks to the marine carbon cycle.

BGD
7, 7271–7314, 2010

2.2 Marine carbon cycle measurements and considerations

Physical and biogeochemical measurements (including marine carbon cycle observations) were collected in the Bering Sea from the US Coast Guard Cutter *Healy* during two cruises in 2008 as part of the Bering Sea Ecological Study (BEST) program (http://www.eol.ucar.edu/projects/best/). During spring (27 March–6 May; HLY 08-02) and summer (3–31 July; HLY 08-03) cruises, 67 and 84 CTD-hydrocast stations were occupied across the Bering Sea shelf on three east to west transects (North Line, Middle Line and South Line) and one north-south transect (Fig. 1; Mathis et al., 2010a). These transects sampled the shallow Coastal (<50 m deep); Middle (~50–100 m deep) and Outer (>100 m deep) domains of the Bering Sea shelf (Fig. 1). At each hydrocast station, conductivity-temperature-depth (CTD) profiles were collected using Seabird SBE-911 sensors while seawater samples were collected from Niskin samplers at representative depths for a suite of biogeochemical measurements (i.e., dissolved oxygen, inorganic nutrients). Shipboard sea-ice observations were retrieved from field reports (http://www.eol.ucar.edu/projects/best/). Sea-ice cover was typically in the range of 90–100% at most stations (with the exception of minor flaw leads; and south of the Pribilof Islands and SE Bering Sea) during the spring cruise while the summer cruise was sea-ice free.

Samples for seawater carbonate chemistry were taken at most CTD/hydrocast stations on both spring and summer cruises. DIC and TA samples were drawn from Niskin samplers into clean 0.3 dm^3 size Pyrex glass reagent bottles, using established gas sampling protocols (Bates et al., 1996a; Dickson et al., 2007). A headspace of <1% of the bottle volume was left to allow for water expansion and all samples were poisoned with 200 µl of saturated $HgCl_2$ solution to prevent biological alteration, sealed and returned to UAF for analysis. DIC was measured by a gas extraction/coulometric technique (see Bates et al., 1996a, b for details), using a VINDTA 3C instrument (Marianda Co.) that controls the pipetting and extraction of seawater samples and a UIC CO_2 coulometer detector. The precision of DIC analyses of this system was typically

BGD
7, 7271–7314, 2010

better than 0.05% (~1 µmol kg^{-1}). TA was determined by potentiometric titration with HCl (see Bates et al., 1996a, b for details) using the VINDTA system. Seawater certified reference materials (CRM's; prepared by A.G. Dickson, Scripps Institution of Oceanography; http://andrew.ucsd.edu/) were analyzed to ensure that the accuracy of DIC and TA was within 0.1% (~2 µmol kg^{-1}).

The complete seawater carbonic acid system (i.e., CO_2, H_2CO_3, HCO_3^-, CO_3^{2-}, H^+) can be calculated from two of four measureable carbonate system parameters (i.e., DIC, TA, pCO_2 and pH), along with temperature and salinity (Zeebe and Wolf-Gladrow, 2001; Dickson et al., 2007). The carbonic acid dissociation constants (pK_1 and pK_2) of Mehrbach et al. (1973), as refit by Dickson and Millero (1997), were used to calculate seawater pCO_2 and other carbonate parameters, using the equations of Zeebe and Wolf-Gladrow (2001). In addition, the CO_2 solubility equations of Weiss (1974), and dissociation constants for borate (Dickson, 1990), and phosphate (Dickson et al., 2007) were used. The calculation of seawater pCO_2 has an error of ~5–10 µatm depending on pK_1 and pK_2 used (i.e., Mehrbach et al. 1973, as refit by Dickson and Millero, 1997; Goyet and Poisson, 1989; Roy et al., 1993; Millero et al., 2006). The difference in calculated seawater pCO_2 using different pK_1 and pK_2 was relatively small (<5 µatm) at temperatures less than 0 °C (Bates, 2006), increasing to ~10–15 µatm in warmer waters (8–12 °C). Overall, the mean difference in calculated seawater pCO_2 was small (<10 µatm) compared to the large range of seawater pCO_2 values (>200 µatm) observed across the Bering Sea shelf.

2.3 Calculation of air-sea CO_2 gas exchange rates

The net air-sea CO_2 flux (F) was determined by the following formula:

$$F = ks(\Delta pCO_2) \quad (1)$$

where k is the transfer velocity, s is the solubility of CO_2 and, ΔpCO_2 is the difference between atmospheric and oceanic partial pressures of CO_2. The ΔpCO_2, or air-sea CO_2 disequilibrium, sets the direction of CO_2 gas exchange while k determines the rate

BGD
7, 7271–7314, 2010

of air-sea CO_2 transfer. Here, gas transfer velocity-wind speed relationships for short-term and long-term wind conditions based on a quadratic (U^2) dependency between wind speed and k (i.e., Wanninkhof, 1992) were used to determine air-sea CO_2 fluxes:

$$k = 0.39{U_{10}}^2(Sc/660)^{-0.5} \quad (2)$$

where U_{10} is wind speed corrected to 10 m, and Sc is the Schmidt number for CO_2. The Schmidt number was calculated using the equations of Wanninkhof (1992) and s (solubility of CO_2 per unit volume of seawater) was calculated from the observed temperature and salinity using the equations of Weiss (1974). Estimates of net air-sea CO_2 flux rates for the Bering Sea shelf were made using two approaches: (1) calculating net air-sea CO_2 flux rates at each hydrocast station, and: (2) using interpolation and extrapolation techniques using interpolation and extrapolation techniques, and a multiple linear regression (MLR) method to produce maps of seawater pCO_2, ΔpCO_2 and air-sea CO_2 flux rates across the Bering Sea with a spatial resolution of 1° and temporal resolution of 1 month (Sect. 2.4).

Net air-sea CO_2 flux rates were computed at each hydrocast station using surface seawater observations and atmospheric pCO_2 data to compute ΔpCO_2 values. Atmospheric pCO_2 data were determined using monthly-resolved latitudinal marine boundary layer atmospheric CO_2 distribution extrapolated to all longitudes. These values were obtained from GLOBALVIEW (http://www.esrl.noaa.gov/gmd/ccgg/globalview/; GLOBALVIEW-CO_2, 2007; Fig. 2), and corrected for water vapor pressure. Synoptic meteorological data (including windspeed) was collected from the USCGC *Healy* during the cruises (Fig. 3). Windspeed data and ΔpCO_2 values (Fig. 4) were then used to determine net air-sea CO_2 flux rates (Fig. 5). Daily averaged 6-hourly wind speed data from the NCEP (National Centers for Environmental Prediction)/NCAR (National Center for Atmospheric Research) reanalysis 2 data assimilation model was also used to calculate k values (http://www.cdc.noaa.gov/cdc/data.ncep.html). NCEP/NCAR Reanalysis 2 (i.e. NNR) data was used in addition to shipboard meteorological data reports in order to allow estimates of air-sea CO_2 fluxes across the

BGD
7, 7271–7314, 2010

Bering Sea to be made. The spatial resolution of the NNR data assimilation model windspeed dataset is 2.5° by 2.5°.

2.4 MLR based model considerations

Inorganic carbon observations of the global ocean typically have limited temporal and spatial coverage compared to other hydrographic properties such as temperature, salinity, dissolved oxygen and inorganic nutrients. Due to data limitations, multiple linear regression (MLR) approaches have often been used to interpolate and extrapolate available inorganic carbon data to ocean basins and the global ocean (e.g., Goyet and Davis, 1997; Goyet et al., 2000; Lee, 2001; Lee et al., 2002; Bates et al., 2006a, b). Similar interpolation and extrapolation techniques have been used to yield global estimates of air-sea CO_2 exchange rates using available surface seawater pCO_2 observations (Takahashi et al., 2002, 2009). In this study, we compared our observed seawater pCO_2 with the data-based seawater pCO_2 climatology of Takahashi et al. (2009) that has a spatial resolution of 4°×5°. In addition, we also compared observed seawater pCO_2 data with a MLR-based model, similar to other studies (e.g., Lee et al., 2000; Lee, 2002; Bates et al., 2006a, b; GLODAP), to produce a data-based seawater pCO_2 climatology map of the Bering Sea with improved spatial resolution (i.e., 1°×1°) .

Using MLR methods, interpolation of DIC and TA distributions from other hydrographic properties such as temperature, salinity, and inorganic nutrients has an uncertainty of ~5–15 µmol kg^{-1} when applied to data below the mixed layer (e.g., Goyet and Davis, 1997; Sabine et al., 1999; Goyet et al., 2000; Sabine and Feely, 2001; Coatanoan et al., 2001; Key et al., 2004). In the mixed layer, the interpolation of DIC and TA has larger uncertainty due to seasonal variability. Here, a MLR-based model is used to interpolate DIC and TA data from observed hydrographic properties using observed seawater carbonate chemistry data collected in the Bering Sea in 2008. Interpolated data were then extrapolated to the entire Bering Sea using climatological hydrographic data from the World Ocean Atlas (WOA, 2005) that has a spatial resolution of 1°×1°, vertically differentiated into 14 layers in the upper 500 m with a temporal

BGD
7, 7271–7314, 2010

resolution of 1 month. Climatological surface seawater pCO_2 maps for the Bering Sea were then calculated from these DIC and TA fields (using the same approach outlined in Sects. 2.2 and 2.3). The seasonal and annual rates of air-sea CO_2 exchange were then compared with data-based seawater pCO_2 climatology maps (Takahashi et al., 2002, 2009).

2.4.1 Interpolation and extrapolation techniques

Several interpolation schemes were investigated using the Bering Sea shelf DIC and TA data including variables such as: temperature (T), salinity (S), oxygen anomaly (O_2a), nitrate (NO_3), phosphate (PO_4), silicate (SiO_4), depth (D), latitude and longitude. The oxygen anomaly was defined as the dissolved oxygen minus the oxygen saturation where the saturation level was calculated from the bottle temperature and salinity data. Different combinations of parameters were tested in order to improve the quality of fit and to reduce the residual errors between the synthetic and measured data. The optimal fit was determined by examining the RMS error, the comparison of the synthetic versus measured data and the spatial pattern of the residuals. We found that the optimal interpolation with the lowest associated uncertainties for DIC and TA (generally for the 0–500 m depth) were a function of the following properties:

$$\mathrm{DIC} = \alpha_1 + \alpha_2 T + \alpha_3 S + \alpha_4 D + \alpha_5 \mathrm{lat} + \alpha_6 \mathrm{NO_3} + \alpha_7 \mathrm{O_2}a + \alpha_8 \mathrm{SiO_4} \quad (3)$$

$$\mathrm{TA} = \beta_1 + \beta_2 T + \beta_3 S + \beta_4 D + \beta_5 \mathrm{lat} + \beta_6 \mathrm{NO_3} + \beta_7 \mathrm{O_2}a + \beta_8 \mathrm{SiO_4} \quad (4)$$

where α and β are the regression coefficients for DIC and TA, respectively. Inclusion of PO_4 or longitude did not improve the regressions. For 2008 spring BEST data, the best-fit MLR regression had an uncertainty of ~12.7 and 8.4 µmol kg^{-1}, for DIC and TA, respectively (Fig. 4). For summer data, the best-fit MLR regression had an uncertainty of ~27.9 and 6.7 µmol kg^{-1} for DIC and TA, respectively (Fig. 4).

MLR regression coefficients were then applied to the World Ocean Atlas 2005 (WOA2005) data for temperature (Locarnini et al., 2006), salinity (Antonov et al., 2006),

BGD
7, 7271–7314, 2010

oxygen (Garcia et al., 2006a) and inorganic nutrient (Garcia et al., 2006b) climatology datasets. This provides extrapolated MLR based maps of mean DIC and TA for the Bering Sea that had a spatial resolution of 1°×1° and temporal resolution of 1 month. In the deep Bering Sea, the model has a vertical resolution of 14 layers in the upper 500 m and typically 4–10 layers (~30–200 m) for the Bering Sea shelf. Surface seawater pCO_2 fields for the Bering Sea were then calculated from MLR based model DIC and TA maps (using the same approach outlined in Sects. 2.2 and 2.3). An important consideration is that modeled MLR maps of DIC, TA and pCO_2 provide a climatological view of seawater carbonate chemistry conditions in the Bering Sea rather than a model simulation of 2008 conditions. The MLR regression coefficients are based on observed DIC, TA and hydrographic data, but the MLR model extrapolation uses climatological, mean values of temperature, salinity, dissolved oygen and inorganic nutrients from the World Ocean Atlas (WOA2005) to compute climatologically based DIC and TA maps.

Errors in the MLR analysis arise from a combination of interpolation and extrapolation errors. Interpolation errors stemmed from the goodness-of-fit of the empirical linear function, where one standard deviation was used to quantify the error. Extrapolation errors arose from applying the regression coefficients to areas of the Bering Sea that have inadequate spatial coverage of data (i.e., open-ocean).

Net air-sea CO_2 flux rates were also computed using surface seawater pCO_2 and ΔpCO_2 maps derived from MLR interpolation and extrapolation. Marine boundary layer atmospheric CO_2 distribution extrapolated to all longitudes were obtained from GLOBALVIEW (GLOBALVIEW-CO_2, 2007). Daily averaged 6-hourly NNR wind speed data was used to calculate k values.

As mentioned earlier, there are many sources of error in an analysis such as this and how they are propagated through the analysis determines how large the error will be on the final air-sea CO_2 flux estimates. Quantifying the error of the interpolation comes directly from the regression models (RMS) where a Monte Carlo method was used to propagate the error from the DIC and TA fields creating a reliable error estimate for the seawater pCO_2 field. For each point, we calculated the pCO_2 a thousand times while

BGD
7, 7271–7314, 2010

randomizing the error at each DIC and TA node. Using an analysis such as this, the mean of the simulation should converge on the estimated pCO_2 field with a reliable error estimate without having to use a brute force method that would maximize the error. Because there was an error estimate for every estimated DIC and TA point from the MLR analysis, there is an associated unique pCO_2 error for every point as well. It was found that the average seawater pCO_2 error for the Bering Sea shelf was 15.2 µatm, relatively small compared to seasonal changes of seawater pCO_2.

3 Results

3.1 Seawater pCO_2 and ΔpCO_2 variability on the Bering Sea shelf

3.1.1 Spring observations of seawater pCO_2 and ΔpCO_2

Spring observations of surface (upper 10 m) seawater pCO_2 ranged from ~180 to ~520 µatm across the Bering Sea shelf. ΔpCO_2 values ranged from ~−200 to ~+130 µatm (Fig. 5) with large spatial variability in the potential for uptake of atmospheric CO_2 or release of CO_2 from the ocean to the atmosphere. In those regions where the potential to uptake atmospheric CO_2 existed, the SE Bering Sea shelf exhibit the strongest air-sea CO_2 gradients with surface seawater pCO_2 values very low (~180–200 µatm) and ΔpCO_2 values highly negative (~−200–180 µatm). Elsewhere across the Bering Sea shelf, particularly between Nunivak Island and the Pribilof Islands, and the outer shelf west of St. Matthew Island, seawater pCO_2 values typically ranged from ~260–330 µatm and ΔpCO_2 values were negative (~−130 to −55 µatm). For comparison, Chen (1993) observed wintertime ΔpCO_2 values of ~−50 to −70 µatm in the region west of St. Matthew Island (~58° N–62° N/171° W to 179° W) in 1983. In most other regions, seawater pCO_2 values from the spring 2008 BEST cruise were similar to atmospheric pCO_2 values. In the Northern Bering Sea shelf, seawater pCO_2 values ranged from ~340–520 µatm. ΔpCO_2 values were positive close to Nunivak Island (~+60–80 µatm), just west of St. Matthew Island (up to +130 µatm), at the

BGD
7, 7271–7314, 2010

outermost shelf stations of the northern line (up to +90 µatm), and at a few deep (off-shelf) Bering Sea stations. As such, these surface waters had the potential to release CO_2 to the atmosphere.

In comparison to the observations, the MLR based model maps of surface seawater pCO_2 indicate that Bering Sea shelf waters typically ranged from ~350–450 µatm (ΔpCO_2 values of ~−50 to +50 µatm) increasing from the inner shelf to the outer shelf and deep Bering Sea (Fig. 6). There were large differences evident between the 2008 spring (and summer) observations and the MLR based model maps. An explanation for the difference is that the MLR model maps, which are based on mean hydrographic values reported in the WOA2005 climatology rather than actual observed hydrography in the Bering Sea in 2008, simulate a "mean" state or climatology for seawater pCO_2 rather than a simulation of 2008 conditions. Thus, observed pCO_2 values were much lower in 2008 for springtime compared to the MLR based Bering Sea seawater pCO_2 climatology.

3.1.2 Summer observations of seawater pCO_2 and ΔpCO_2

Summertime observations of surface seawater pCO_2 exhibited a greater range (~130 to ~640 µatm) than springtime with most of the Bering Sea shelf strongly undersaturated with respect to the atmospheric (Fig. 5). The lowest surface seawater pCO_2 values were observed in the "*green belt*" of the middle and outer shelf between the Northern and Southern Bering Sea shelf (between Nunivak Island and the Pribilof Islands). In this regions, ΔpCO_2 values ranged from ~−250 to −50 µatm and surface waters had a very strong potential to uptake atmospheric CO_2. In the SE Bering Sea, in contrast to the "*green belt*" of the shelf, surface seawater pCO_2 had increased from springtime values of ~180–200 µatm to ~330–425 µatm reducing the driving force for uptake of atmospheric CO_2. At the innermost stations of the Northern Bering Sea shelf and just south of the Pribilof Islands, surface seawater pCO_2 had high values (up to ~670 µatm). Thus in contrast with much of the shelf, these relatively small areas had a strong potential to release CO_2.

BGD
7, 7271–7314, 2010

In comparison to the observations, the MLR based maps indicate that summertime Bering Sea shelf waters typically ranged from ~200–300 µatm (ΔpCO_2 values of ~−150 to −100 µatm), increasing from the inner shelf to the outer shelf and deep Bering Sea (Fig. 6), and also in the SE Bering Sea shelf region. Observed pCO_2 values were much lower in 2008 in summertime compared to the MLR based Bering Sea seawater pCO_2 climatology.

3.2 Air-sea CO_2 fluxes on the Bering Sea shelf

3.2.1 Springtime air-sea CO_2 fluxes

In springtime, potential air-sea CO_2 flux rates in the Northern Bering Sea shelf varied between ~0 and −10 mmol CO_2 m^{-2} d^{-1} (negative values denote ocean CO_2 sink), with the outer stations exhibiting the potential for efflux of CO_2 up to ~+25 mmol CO_2 m^{-2} d^{-1} (Fig. 7). In the Middle Bering Sea shelf, potential air-sea CO_2 flux rates were close to neutral (between ~0 and −10 mmol CO_2 m^{-2} d^{-1}) particularly to the west of St. Matthew Island. There were localized areas of surface water that acted as potentially larger sinks of CO_2 (~170° W) with the strongest potential efflux closest to shore (i.e., Nunivak Island; Fig. 7). In these regions, an important caveat is that the presence of sea-ice forms a barrier to air-sea gas exchange. Given that the sea-ice % cover varied between ~90% and 100% and open water area was <10%, the actual air-sea CO_2 flux rates would likely be much smaller (<0–3 mmol CO_2 m^{-2} d^{-1}) similar to other studies of sea-ice covered Arctic Ocean waters (e.g., Bates, 2006; Bates and Mathis, 2009). We recognize however that some studies suggest that sea-ice allows gas exchange (Gosink et al., 1978; Semiletov et al., 2004; Delille et al., 2007; Nagurnyi, 2008) and so wintertime/springtime air-sea CO_2 flux rates may be higher during sea-ice covered conditions.

Over the Southern Bering Sea shelf, where sea-ice cover was much less, surface waters between Nunavak Island and the Pribilof Islands had modest influx rates of ~−10 to −25 mmol CO_2 m^{-2} d^{-1}. In comparison, our MLR based model climatological maps

BGD
7, 7271–7314, 2010

showed mostly low rates of air-sea CO_2 exchange (−10 to +10 mmol CO_2 m^{-2} d^{-1}) across much of the shelf regions, with higher efflux rates occuring in the outershelf (particularly north of St. Matthew Island as in observations), and also offshore (Fig. 6).

3.2.2 Summertime air-sea CO_2 fluxes

During the summertime cruise, sea-ice was absent and the Bering Sea shelf had transitioned from mostly neutral conditions to a stronger oceanic sink for CO_2. In the Northern Bering Sea, the rates of air-sea CO_2 flux rates varied from −15 to −60 mmol CO_2 m^{-2} d^{-1} (Fig. 7). The exception to this general observation was a small region of efflux at the innermost shelf station (up to +30 mmol CO_2 m^{-2} d^{-1}). Previous studies have suggested that the nearshore waters were influenced by river runoff (Mathis et al., 2010) which tend to have high pCO_2 values (e.g., Salisbury et al., 2008). Along the shelf to the west of St. Matthew Island south to the Pribilof Islands in the region of the Bering Sea "*green belt*", air-sea CO_2 flux rates varied, mostly between −15 and −60 mmol CO_2 m^{-2} d^{-1} with some areas of higher influx (−120 mmol CO_2 m^{-2} d^{-1}) between Nunivak Island and the Pribilof Islands. However, close to the Pribilof Islands, air-sea CO_2 flux rates were much reduced (−5 to −25 mmol CO_2 m^{-2} d^{-1}), but a region of CO_2 efflux was observed south of the Pribilof Islands (up to +60 mmol CO_2 m^{-2} d^{-1}). In the SE Bering Sea, air-sea CO_2 flux rates were close to neutral with no net influx or efflux of CO_2. In comparison, our MLR model of climatological air-sea CO_2 flux showed that much of the Bering Sea shelf was typically a modest sink for CO_2 (with air-sea CO_2 flux rates of −10 to −30 mmol CO_2 m^{-2} d^{-1}). In similarity to observational based estimates, there was an air-sea CO_2 efflux offshore and at the nearshore stations (Fig. 6).

BGD
7, 7271–7314, 2010

4 Discussion

4.1 Potential controls on seawater pCO_2 and air-sea CO_2 gas exchange across the Bering Sea

There are many physical and biological processes that can influence seawater pCO_2 and air-sea CO_2 gas exchange but the major factors include warming/cooling, the balance of evaporation and precipitation, vertical and horizontal mixing (including entrainment/detrainment; vertical diffusion, and advection), biological uptake/release of CO_2 and alkalinity (including surface layer net pelagic phytoplankton primary production and calcification, export production, subsurface remineralization and the balance of net autrtrophy/heterotrophy; Ducklow and McAllister, 2005), and the process of gas exchange itself. In nearshore and shallow coastal seas, the contributions of river runoff and sedimentary uptake/release of CO_2 and alkalinity (e.g., Thomas et al., 2009) have more importance. In seasonally sea-ice covered waters, sea-ice can act as a barrier to gas exchange (note that there is significant disagreement on this process, Gosink, 1976; Delille et al., 2003; Semiletov et al., 2007), carbon export can be facilitated via brine rejection during sea-ice formation (e.g., Omar et al., 2005) and sea-ice melt properties and sea-ice biota can significantly modify surface inorganic carbon properties. Here, we examine the effect of temperature change and ocean biology on seawater pCO_2 and air-sea CO_2 gas exchange rates on the Bering Sea shelf following a simple empirical analysis used to determine the primary controls on temporal and spatial variability of global ocean pCO_2 (Takahashi et al., 2002, 2009).

As shown in other studies, the Bering Sea shelf exhibits seasonal spring to summer warming of up to 10 °C. In order to remove the temperature effect from the observed pCO_2, seawater pCO_2 values are normalized to a constant temperature of 0 °C using the equation (Takahashi et al., 2002):

$$pCO_2 \text{ at } 0°C = {pCO_2}^{obs} \times \exp[(0.0423(T^{obs} - 0°C))] \quad (5)$$

where T^{obs} is the observed temperature. This normalization procedure accounts for the thermodynamic effect of warming/cooling on seawater pCO_2 which has been

BGD
7, 7271–7314, 2010

experimentally determined at about 4.23% change in pCO_2 per ˚C change (Takahashi et al., 1993).

Seawater pCO_2 temperature normalization can be used to assess the impact of temperature and ocean biology on the seasonal changes in pCO_2 observed over the Bering Sea shelf between spring and summer. For regional interpretation, we compute the mean observed seawater pCO_2 difference between spring and summer ($\delta pCO_2^{\text{spring-summer}}$) and change in pCO_2 due to spring-summer changes in temperature (i.e., $\delta pCO_2^{\text{temperature}}$ computed using Eq. 6) for five different regions of the Bering Sea shelf, including; (1) the North Line; (2) the Middle Line; (3) between Nunavak Island and Pribilof Islands, (4) south of the Probilof Islands, and; (5) SE Bering Sea shelf. The unknown term, $\delta pCO_2^{\text{biology}}$, which is the change in pCO_2 due to spring-summer changes in ocean biology, is solved from the following equation:

$$\delta pCO_2^{\text{spring-summer}} = \delta pCO_2^{\text{temperature}} + \delta pCO_2^{\text{biology}} \quad (6)$$

This approach follows the empirically based method of Takahashi et al. (2002) in which the term $\delta pCO_2^{\text{biology}}$, approximates the "net biology" effect or the net balance of photosynthesis and respiration or net community production (NCP). An important caveat is that this term also includes minor contributions from alkalinity changes due to $CaCO_3$ production/dissolution and nitrate utilization, and vertical/horizontal contributions from mixing with subsurface waters or offshore waters, and air-sea CO_2 gas exchange. Salinity changes as a result of evaporation and precipitation also have very minor impact on seawater pCO_2 since DIC and total alkalinity are changed in equal proportion. Sea-ice melt and river runoff were also considered very minor in nature. The inherently simple construct of this approach allows a general view of how seasonal warming or "net biology" (i.e., NCP) influences the ocean CO_2 sink and sources status of the Bering Sea shelf. As in the Takahashi et al. (2002) approach, we assess whether the effects of seasonal temperature changes on seawater pCO_2 exceeds the biological effect (e.g., as in the North Atlantic Ocean) or the opposite (i.e., "net biology">temperature; e.g., Ross Sea).

BGD
7, 7271–7314, 2010

Over the Northern and Central Bering Sea shelf, there was a seasonal (i.e., spring to summer) drawdown of surface seawater pCO_2 of ~100 µatm (Figs. 8 and 9). In the North Line, mean surface seawater pCO_2 declined seasonally from 387.5±85.2 µatm to 283.8±123.5 µatm. Similarly in the Middle Line and between Nunivak Island and the Pribilof Islands, mean surface seawater pCO_2 declined seasonally from 367.4±56.2 µatm to 219.0±58.0 µatm, and 329.0±35.9 µatm to 270.8±108 µatm, respectively. In comparison to observed seawater pCO_2 changes, temperature corrected seawater pCO_2 decreased seasonally by ~200 µatm (Figs. 8 and 9), and up to 300 µatm lower within the "*green belt*" area by the summertime. Thus, in these regions, the "net biology" effect strongly dominated the seasonal change in surface seawater pCO_2 compared to warming (Fig. 10). The 2008 BEST data indicates that the "net biology" effect seasonally decreases seawater pCO_2 by ~150 to ~230 µatm (Fig. 10) with this drawdown only partially compensated for by an increase in seawater pCO_2 due to seasonal warming. For comparison, the Takahashi et al. (2002) climatology suggests that the seasonal drawdown of seawater pCO_2 associated with "net biology" effects is ~130–170 µatm. In addition, Mathis et al. (2010a) showed that large seasonal drawdown of DIC results from high rates of NCP particularly within the "*green belt*" area of the Bering Sea shelf. Our data provides further evidence that "net biology" dominates the seasonal drawdown of seawater pCO_2 for large areas of the Bering Sea shelf. Indeed, seasonal "net biology" effects or spring-summer NCP shifts much of the Bering Sea shelf from a neutral CO_2 sink/source status in spring to a strong sink for CO_2 by summertime.

In contrast to the Northern and Central Bering Sea shelf, warming appears to dominate the seasonal changes of seawater pCO_2 for small areas south of the Pribilof Islands and in the SE Bering Sea shelf region. In these two regions, mean surface seawater pCO_2 increased seasonally from 297.1±33.0 µatm to 338.2±137.8 µatm, and from 293.0±55.2 µatm to 324.9±63.2 µatm, respectively. In these two regions, temperature corrected seawater pCO_2 decreased seasonally by less than ~50 µatm (Fig. 9). South of the Pribilof Islands, the seasonal "net biology" effect of ~50 µatm was about

BGD
7, 7271–7314, 2010

half of the increase of seawater pCO_2 caused by warming (Fig. 10). In the SE Bering Sea shelf region, there was no seasonal "net biology" effect, and the increase in observed seawater pCO_2 was due to warming only. Surface nitrate data in the SE Bering Sea shelf region were typically below 1 µmol kg^{-1} for both spring and summer cruises. This suggests that the typical "spring" phytoplankton bloom observed in the SE Bering Sea shelf had occurred earlier than the spring cruise, and that ocean biology had minimal impact on seawater pCO_2 and air-sea CO_2 fluxes in the spring-summer period. This region also exhibits episodic coccolithophore blooms (e.g., Merico et al., 2004, 2006) that can increase seawater pCO_2 (e.g., Bates et al., 1996; Harley et al., 2010). However, there was no evidence in the BEST alkalinity (TA) data for significant impact of coccolithophore blooms in 2008. In all regions, there were no statistically significant changes in salinity normalized TA (i.e., here defined as nTA+NO_3 to account for the contribution of nitrate to alkalinity; Brewer and Goldman, 1978) from spring to summer (Fig. 11). nTA+NO_3 values were slightly lower south of the Pribilof Islands and in the SE Bering Sea shelf compared to other regions which suggests that if coccolithophores contributed significantly to the "spring" phytoplankton bloom, this occurred earlier than the spring cruise. In summary, in contrast to most of the Bering Sea shelf, seasonal warming shifted localized areas of the shelf from minor/neutral CO_2 sink status to neutral/minor CO_2 source status.

4.2 2008 BEST data in context of seasonal changes in pCO_2 and annual air-sea CO_2 fluxes

On the Bering Sea shelf, previous studies have shown inorganic carbon data distributions (e.g., Park et al., 1974; Codispoti et al., 1982, 1986; Mathis et al., 2010a) but there is very limited data on seawater pCO_2 (Kelley and Hood, 1971; Chen, 1993). Several studies report Northern Bering Sea shelf seawater pCO_2 but these data were collected north of St. Lawrence Island (Murata and Takizawa, 2002; Chen and Gao, 2007) outside the domain of our study. The Takahashi et al. (2009) seawater pCO_2 climatology shows a seasonal change of ~50–80 µatm for the Bering Sea shelf with

BGD
7, 7271–7314, 2010

a spring-summer drawdown (Fig. 12) that causes the shelf to act as a CO_2 sink (~1–2 mol C m^{-2} yr^{-1}). However, an important caveat is that the seawater pCO_2 climatology is based on very limited data (1 cruise), and thus it is difficult to draw firm conclusions about the seasonal and annual CO_2 sink-source status of the Bering Sea shelf.

The Takahashi et al. (2009) seawater pCO_2 climatology has four 4° × 5° areas that overlie the Bering Sea shelf (Fig. 12). For July, average ΔpCO_2 values range from −20.8 to −44.7 µatm for these four. In contrast, the 2008 BEST summer mean ΔpCO_2 values ranged from −110.8 to −170.4 µatm for the same areas, indicating that the shelf was much more strongly undersaturated than the seawater pCO_2 climatology suggests. As a consequence, the mean July air-to-sea CO_2 fluxes calculated here were about 5 times higher (~−16.3 to −24.2 mmol m^{-2} d^{-1}) than the Takahashi et al. (2009) seawater pCO_2 climatology.

Early model studies of Walsh and Dieterle (1994), using data collected by Codispoti et al. (1986), indicated that the annual CO_2 sink was ~4.3 mol C m^{-2} yr^{-1} (Table 1). Based on the flux reported by Walsh and Dieterle (1994), we calculated that the net annual CO_2 sink for the Bering Sea shelf was ~3.4 Tg C yr^{-1}. In this and subseqent calculations, we assumed that the surface area of the Bering Sea shelf was ~500 000 km^2, that sea-ice free, open water conditions were typically present for 180 days a year, and that there was not significant gas exchange during sea-ice cover. More recently, Chen and Borges (2009) summarized coastal air-sea CO_2 fluxes, reporting springtime and summertime fluxes of ~−1.2 mmol C m^{-2} d^{-1} (Nedashkovskii and Sapozhnikov, 2001) and 0.66 mmol C m^{-2} d^{-1} (Codispoti et al., 1986), respectively. If we scale up these flux rates, accounting for Bering Sea surface area and period of open water conditions, we estimate a net annual CO_2 sink of ~11 Tg C yr^{-1}. Similarly, scaling our observations and the climatology of Takahashi et al. (2009), we compute that the Bering Sea shelf CO_2 sink was 157±35 Tg C yr^{-1} and ~36 Tg C yr^{-1}, respectively (Table 1). The primary difference between the 2008 BEST datasets and Takahashi et al. (2009) seawater pCO_2 climatology relates to the much larger undersaturation observed in surface waters during summertime (Fig. 12). Our annnual estimate of 157 Tg C yr^{-1}, compares to

BGD
7, 7271–7314, 2010

the estimates for the entire Bering Sea of 200 Tg C yr^{-1} reported by Chen et al. (2004).

There are many caveats in scaling any of the above flux data to annual CO_2 flux rates and caution must be considered in undertaking this scaling up and interpreting such results. If the 2008 BEST datasets are indeed representative of typical conditions, then the Bering Sea shelf is a much larger CO_2 sink than previously thought. At the very least, such uncertainties in providing an accurate assessment of the annual CO_2 sink-source status of the Bering Sea shelf, requires future long-term monitoring efforts for this important shelf region. It should also be noted that an extensive coccolithophore bloom was not observed in the Bering Sea in 2008, but this phenomena has been observed in prior years (e.g., Merico et al., 2004, 2006) and in 2009. Since coccolithophore calcification can result in an increase of seawater pCO_2 (e.g., Bates et al., 1996; Harley et al., 2010), the Bering Sea shelf CO_2 sink may be much reduced in those years with significant coccolithophore bloom events.

5 Conclusions

Spring observations in 2008 of surface seawater pCO_2 ranged from ~180 to ~520 µatm across the Bering Sea shelf but the presence of sea-ice and relatively small ΔpCO_2 gradients suggest that much of the Bering Sea shelf was close to neutral in terms of CO_2 sink-source status. Summertime observations of surface seawater pCO_2 exhibited a greater range (~130 to ~640 µatm) than springtime with most of the Bering Sea shelf strongly undersaturated with respect to the atmosphere, and the Bering Sea shelf had transitioned from mostly neutral conditions to a stronger oceanic sink for atmospheric CO_2. Our data further suggests that biological processes (or the NCP of the shelf) dominates the seasonal drawdown of seawater pCO_2 for large areas of the Bering Sea shelf during late spring and summer, with the effect partly countered by seasonal warming, particularly in the Southeastern Bering Sea. Thus seasonal "net biology" effects strongly shift much of the Bering Sea shelf from a neutral CO_2 sink/source status in spring to a strong oceanic sink for CO_2 by summertime. Although

BGD
7, 7271–7314, 2010

our data does not include fall or winter data, we anticipate that late season mixing restores the Bering Sea shelf to near neutral CO_2 sink status before sea-ice provides a barrier to further CO_2 gas exchange. In small areas of the Bering Sea shelf south of the Pribilof Islands and in the SE Bering Sea, seasonal warming is the dominant influence on seawater pCO_2, shifting localized areas of the shelf from minor/neutral CO_2 sink status to neutral/minor CO_2 source status, in contrast to much of the surrounding Bering Sea shelf. Overall, the Bering Sea shelf appears to be a stronger sink for atmospheric CO_2 than previously suggested by the Takahashi et al. (2009) seawater pCO_2 climatology. Given that Bering Sea shelf is the largest US coastal shelf sea, we suggest that future long-term monitoring of the region is critical for assessments of the contribution of the Bering Sea shelf to regional carbon budgets and evaluation of seasonal and interannual variability in response to natural and anthropogenically influenced climate change.

Acknowledgements. The authors wish to thank the officers and crew of the USCGC *Healy* for their logisitical support as well as our collegues in the BEST-BSIERP project for allowing us to make these measurements. We would like to specifically thank the hydrographic team at NOAA-PMEL including Phyllis Stabeno, Calvin Moordy, Nancy Kachel, and the many others who helped in sample collection and provided high quality temperature, salinity, oxygen and nutrient data. The work presented in this paper was supported by the Bureau of Ocean Energy Management, Regulation and Enforcement and the Coastal Marine Institute at the University of Alaska Fairbanks under Agreement M08AC12645.

References

Antonov, J. I., Locarnini, R. A., Boyer, T. P., Mishonov, A. V., and Garcia, H. E.: World Ocean Atlas 2005, Volume 2: Salinity, edited by: Levitus, S., NOAA Atlas NESDIS 62, US Government Printing Office, Washington, DC, 182 pp., 2006.

Banse, K. and English, D. C.: Comparing phytoplankton seasonality in the Eastern and Western subarctic Pacific and the Western Bering Sea, Prog. Oceanogr., 43, 235–288, 1999.

Bates, N. R.: Air-sea CO_2 fluxes and the continental shelf pump of carbon in the

BGD

7, 7271–7314, 2010

Chukchi Sea adjacent to the Arctic Ocean, J. Geophys. Res.-Oceans, 111, C10013, doi:10.129/2005JC003083, 2006.
Bates, N. R. and Mathis, J. T.: The Arctic Ocean marine carbon cycle: evaluation of air-sea CO_2 exchanges, ocean acidification impacts and potential feedbacks, Biogeosciences, 6, 2433–2459, doi:10.5194/bg-6-2433-2009, 2009.
Bates, N. R., Michaels, A. F., and Knap, A. H.: Seasonal and interannual variability of the oceanic carbon dioxide system at the US JGOFS Bermuda Atlantic Time-series Site, Deep-Sea Res. Pt. II, 43(2–3), 347–383, doi:10.1016/0967-0645(95)00093-3, 1996a.
Bates, N. R., Michaels, A. F., and Knap, A. H.: Alkalinity changes in the Sargasso Sea: Geochemical evidence of calcification? Mar. Chem., 51(4), 347–358, doi:10.1016/0304-4203(95)00068-2, 1996b.
Bates, N. R., Pequignet, A. C., and Sabine, C. L.: Ocean carbon cycling in the Indian Ocean: II. Estimates of net community production, Global Biogeochem. Cy., 20(3), GB3021, doi:10.1029/2005GB002492, 2006.
Bates, N. R., Pequignet, A. C., and Sabine, C. L.: Ocean carbon cycling in the Indian Ocean: 1. Spatiotemporal variability of inorganic carbon and air-sea CO_2 gas exchange, Global Biogeochem. Cy., 20(3), GB3020, doi:10.1029/2005GB002491, 2006.
Bond, N. A., Overland, J. E., Spillane, M., and Stabeno, P.: Recent shifts in the state of the North Pacific, Geophys. Res. Lett., 30(23), 2183, doi:10.1029/2003GL018597, 2003.
Bond, N. A. and Overland, J. E.: The importance of episodic weather events to the ecosystem of the Bering Sea shelf, Fish. Oceanogr., 14(2), 97–111, 2005.
Brewer, P. G. and Goldman, J. C.: Alkalinity changes generated by phytoplankton growth, Limnol. Oceanogr., 21(1), 108–117, 1976.
Broerse, A. T. C., Tyrell, T., Young, J. R., Poulton, A. J., Merico, A., Balch, W. M., and Miller, P. I.: The cause of bright waters in the Bering Sea in winter, Cont. Shelf Res., 23, 1579–1596, 2003.
Chen, C. T.-A.: Carbonate chemisrty of the wintertime Bering Sea marginal ice zone, Cont. Shelf Res., 13(1), 67–87, 1993.
Chen, C. T. A. and Borges, A. V.: Reconciling opposing views on carbon cycling in the coastal ocean: continental shelves as sinks and near-shore ecosystems as sources of atmospheric CO_2, Deep-Sea Res. Pt. II, 56(8–10), 578–581, doi:10.1016/j.dsr2.2009.01.001, 2009.
Chen, C. T.-A., Andreev, A., Kim, K. R., and Yamamoto, M.: Roles of continental shelves and marginal seas in the biogeochemical cycles of the North Pacific Ocean, J. Oceanogr., 60(1),

BGD
7, 7271–7314, 2010

17–44, 2004.
Chen, L. and Gao, Z.: Spatial variability in the partial pressures of CO_2 in the Northern Bering and Chukchi seas, Deep-Sea Res. Pt. II, 54, 2619–2629, 2007.
Coatanoan, C., Goyet, C., Gruber, N., Sabine, C. L., and Warner, M.: Comparison of two approaches to quantify anthropogenic CO_2 in the ocean: results from the northern Indian Ocean, Global Biogeochem. Cy., 15, 11–25, 2001.
Codispoti, L. A., Friederich, G. E., Iverson, R. L., and Hood, D. W.: Temporal changes in the inorganic carbon system of the Southeastern Bering Sea during spring 1980, Nature, 296, 242–245, 1982.
Codispoti, L. A., Friederich, G. E., and Hood, D. W.: Variability in the inorganic carbon system over the Southeastern Bering Sea shelf during spring 1980 and spring-summer 1981, Cont. Shelf Res., 5, 133–160, 1986.
Comiso J. C., Parkinson, C. L., Gersten, R., and Stock, L.: Accelerated decline in the Arctic sea ice cover, Geophys. Res. Lett., 35, L01703, doi:10.1029/2007GL031972, 2008.
Delille, B., Jourdain, B., Borges, A. V., Tison, J.-L., and Delille, D.: Biogas (CO_2, O_2, dimethylsulfide) dynamics in spring Antarctic fast ice, Limnol. Oceanogr., 52, 1367–1379, 2007.
Dickson, A. G. and Millero, F. J.: A comparison of the equilibrium constants for the dissociation of carbonic acid in seawater media, Deep-Sea Res., 34, 1733–1743, 1987.
Dickson, A. G., Sabine, C. L., and Christian, J. R.: Guide to best practices for ocean CO_2 measurements, Sidney, British Columbia, North Pacific Marine Science Organization, PICES Special Publication 3, 2007.
Ducklow, H. W. and McAllister, S. L.: Biogeochemistry of carbon dioxide in the coastal oceans, in: The Sea, Volume 13, The Global Coastal Ocean-Multiscale Interdisciplinary Processes, edited by: Robinson, A. R. and Brink, K., J. Wiley and Sons, NY, 2005.
Garcia, H. E., Locarnini, R. A., Boyer, T. P., and Antonov, J. I.: World Ocean Atlas 2005, Volume 3: Dissolved Oxygen, Apparent Oxygen Utilization, and Oxygen Saturation, edited by: Levitus, S., NOAA Atlas NESDIS 63, US Government Printing Office, Washington, DC, 342 pp., 2006a.
Garcia, H. E., Locarnini, R. A., Boyer, T. P., and Antonov, J. I.: World Ocean Atlas 2005, Volume 4: Nutrients (phosphate, nitrate, silicate), edited by: Levitus, S., NOAA Atlas NESDIS 64, US Government Printing Office, Washington, DC, 396 pp., 2006b.
GLOBALVIEW-CO_2: Cooperative Atmospheric Data Integration Project for Carbon Dioxide, 2007, CD-ROM, NOAA CMDL, Boulder, CO, also available on Internet via anonymous FTP

BGD
7, 7271–7314, 2010

to ftp.cmdl.noaa.gov, Path: ccg/co2/GLOBALVIEW, 2007.
Gosink, T. A., Pearson, J. G., and Kelley, J. J.: Gas movement through sea ice, Nature, 263, 41–42, doi:10.1038/263041al, 1976.
Goyet, C. and Poisson, A. P.: New determination of carbonic acid dissociation constants in seawater as a function of temperature and salinity, Deep-Sea Res., 36, 1635–1654, 1989.
Goyet, C. and Davis, D.: Estimation of total CO_2 concentration throughout the water column, Limnol. Oceanogr., 44, 859–877, 1997.
Grebmeier, J. M., Cooper, L. W., Feder, H. M., and Sirenko, B. I.: Ecosystem dynamics of the Pacific-influenced Northern Bering and Chukchi Seas in the Amerasian Arctic, Prog. Oceanogr., 71(2–4), 331–361, 2006a.
Grebmeier, J. M., Overland, J. E., Moore, S. E., Farley, E. V., Carmack, E. C., Cooper, L. W., Frey, K. E., Helle, J. H., McLaughlin, F. A., and McNutt, S. L.: A major ecosystem shift in the Northern Bering Sea, Science, 311(5766), 1461–1464, 2006b.
Grebmeier, J. M., Bates, N. R., and Devol, A.: Continental Margins of the Arctic Ocean and Bering Sea, in: North American Continental Margins: A Synthesis and Planning Workshop, edited by: Hales, B., Cai, W.-J., Mitchell, B. G., Sabine, C. L., and Schofield, O., 120 pp., 61–72, 2008.
Hansell, D. A., Goering, J. J., Walsh, J. J., McRoy, C. P., Coachman, L. K., and Whitledge, T. E.: Summer phytoplankton production and transport along the shelf break front in the Bering Sea, Cont. Shelf Res., 9, 1085–1104, 1989.
Harley, J., Borges, A. V., Van Der Zee, C., Delille, B., Godi, R. H. M., Schiettecatte, L.-S., Roevros, N., Aerts, K., Plapernat, P.-E., Rebreanu, L., Groom, S., Daro, M.-H., Van Grieken, R., and Chou, L.: Biogeochemical study of coccolithophore bloom in the northern Bay of Biscay (NE Atlantic Ocean) in June 2004, Prog. Occeanogr., 86, 317–336, doi:10.1016/j.pocean.23010.04.029, 2010.
Hollowed, A. B., Hare, S. R., and Wooster, W. S.: Pacific Basin climate variability and patterns of Northeast Pacific marine fish populations, Prog. Oceanogr., 49, 257–282, 2001.
Hunt, G. L., Stabeno, P., Walters, G., Sinclair, E., Brodeur, R. D., Napp, J. M., and Bond, N. A.: Climate change and control of the Southeastern Bering Sea pelagic ecosystem, Deep-Sea Res. Pt. II, 49(26), 5821–5853, 2002.
Kelley, J. J. and Hood, D. W.: Carbon dioxide in the surface water of the ice-covered Bering Sea, Nature, 229, 37–39, 1971.
Key, R. M., Kozyr, A., Sabine, C. L., Lee, K., Wanninkhof, R., Bullister, J. L., Feely, R. A.,

BGD
7, 7271–7314, 2010

Millero, F. J., Mordy, C., and Peng, T.-H.: A global ocean carbon climatology: results from Global Data Analysis Project (GLODAP), Global Biogeochem. Cy., 18, GB4031, doi:10.1029/2004GB002247, 2004.
Lee, K.: Global net community production estimated from the annual cycle of surface water total dissolved inorganic carbon, Limnol. Oceanogr., 46(6), 1287–1297, 2001.
Lee, K., Karl, D. M., Wanninkhof, R., and Zhang, J. Z.: Global estimates of net carbon production in the nitrate-depleted tropical and subtropical oceans, Geophys. Res. Lett., 29(19), 1907, 2002.
Locarnini, R. A., Mishonov, A. V., Antonov, J. I., Boyer, T. P., and Garcia, H. E.: World Ocean Atlas 2005, Volume 1: Temperature, edited by: Levitus, S., NOAA Atlas NESDIS 61, US Government Printing Office, Washington, DC, 182 pp., 2006.
Macklin, S. A., Hunt, G. L., and Overland, J. E.: Collaborative research on the pelagic ecosystem of the Southeastern Bering Sea shelf, Deep-Sea Res. Pt. II, 49(26), 5813–5819, 2002.
Mathis, J. T., Cross, J. N., Bates, N. R., Bradley Moran, S., Lomas, M. W., Mordy, C. W., and Stabeno, P. J.: Seasonal distribution of dissolved inorganic carbon and net community production on the Bering Sea shelf, Biogeosciences, 7, 1769–1787, doi:10.5194/bg-7-1769-2010, 2010a.
Mathis, J. T., Cross, J., and Bates, N. R.: Coupling primary production and terrestrial runoff to ocean acidification and carbonate mineral suppression in the Eastern Bering Sea, J. Geophys. Res., 2010b.
McRoy, C. P. and Goering, J. J.: The influence of ice on the primary productivity of the Bering Sea, in: Oceanography of the Bering Sea with Emphasis on Renewable Resources, edited by: Hood, D. W. and Kelley, E. J., Univ. of Alaska, Fairbanks, 403–421, 1974.
Mehrbach, C., Culberson, C. H., Hawley, J. E., and Pytkowicz, R. M.: Measurement of the apparent dissociation constants of carbonic acid in seawater at atmospheric pressure, Limnol. Oceanogr., 18, 897–907, 1973.
Merico, A., Tyrrell, T., Lessard, E. J., Oguz, T., Stabeno, P. J., Zeeman, S. I., and Whitledge, T. E.: Modelling phytoplankton succession on the Bering Sea role of climate influences and trophic interactions in generating *Emiliania huxleyi* blooms 1997–2000, Deep-Sea Res. Pt. I, 51(12), 1803–1826, 2004.
Merico, A., Tyrrell, T., and Cokacar, T.: Is there any relationship between phytoplankton seasonal dynamics and the carbonate system? J. Marine Syst., 59(1–2), 120–142, 2006.
Midorikawa, T., Umeda, T., Hiraishi, N., Ogawa, K., Nemoto, K., Kubo, N., and Ishii, M.: Estima-

BGD
7, 7271–7314, 2010

tion of seasonal net community production and air-sea CO_2 flux based on the carbon budget above the temperature minimum layer in the Western subarctic North Pacific, Deep-Sea Res. Pt. I, 49(2), 339–362, 2002.

Millero, F. J., Graham, T. B., Huang, F., Bustos-Serrano, H., and Pierrot, D.: Dissociation constants of carbonic acid in seawater as a function of salinity and temperature, Mar. Chem., 100, 80–94, 2006.

Murata A. and Takizawa T.: Impact of a coccolithophorid bloom on the CO_2 system in surface waters of the Eastern Bering Sea shelf, Geophys. Res. Lett., 29(11), 1547, 2002.

Murphy, P. P., Nojiri, Y., Harrison, D. E., and Larkin, N. K.: Scales of spatial variability for surface ocean pCO_2 in the Gulf of Alaska and Bering Sea: toward a sampling strategy, Geophys. Res. Lett., 28(6), 1047–1050, 2001.

Nagurnyi, A. P.: On the role of Arctic sea-ice in seasonal variability of carbon dioxide concentration in Northern Latitudes, Russ. Meteor. Hydrol., 33(1), 43–47, 2008.

Napp, J. M. and Hunt, G. L.: Anomalous conditions in the South-Eastern Bering Sea 1997: linkages among climate, weather, ocean, and biology, Fish. Oceanogr., 10, 61–68, 2001.

Nedashkovskii, A. P. and Sapozhnikov, V. V.: Estimation of the CO_2 fluxes through the ocean-atmosphere boundary by hydrochemical parameters in the western part of the Bering Sea, Oceanology, 41(3), 351–359, 2001.

Okkonen, S. R., Schmidt, G. M., Cokelet, E. D., and Stabeno, P. J.: Satellite and hydrographic observations of the Bering Sea "Green Belt", Deep-Sea Res. Pt. II, 51(10–11), 1033–1051, 2004.

Omar, A., Johannessen, T., Bellerby, R. G. J., Olsen, A., Anderson, L. G., and Kivimäe, C.: Sea ice and brine formation in Storfjorden: implications for the Arctic wintertime air-sea CO_2 flux, in: The Nordic Seas: An Integrated Perspective: Oceanography, Climatology, Biogeochemistry, and Modeling, edited by: Drange, H., Dokken, T., Furevik, T., Gerdes, R., and Berger, W., Geoph. Monog., 158, 177–187, 2005.

Park, P. K., Gordon, L. I., and Alvarez-Borego, S.: The carbon dioxide system of the Bering Sea, in: Oceanography of the Bering Sea, edited by: Hood, D. W. and Kelley, J. J., Fairbanks, AK, Institute of marine Sciences, University of Alaska, 107–147, 1974.

Piepenburg, D.: Recent research on Arctic benthos: common notions need to be revised, Polar Biol., 28(10), 733–755, 2005.

Rho, T. and Whitledge, T. E.: Characteristics of seasonal and spatial variations of primary production over the Southeastern Bering Sea shelf, Cont. Shelf Res., 27(20), 2556–2569,

BGD
7, 7271–7314, 2010

2007.
Ridgwell, A., Zondervan, I., Hargreaves, J. C., Bijma, J., and Lenton, T. M.: Assessing the potential long-term increase of oceanic fossil fuel CO_2 uptake due to CO_2-calcification feedback, Biogeosciences, 4, 481–492, doi:10.5194/bg-4-481-2007, 2007.
Riebesell, U., Zondervan, I., Rost, B., Tortell, P. D., Zeebe, R. E., and Morel, F. M. M.: Reduced calcification of marine plankton in response to increased atmospheric CO_2, Nature, 407, 364–367, 2000.
Robertson, J. E., Turner, D. R., Holligan, P. M., Watson, A. J., Boyd, P., Fernandez, E., and Finch, M.: The impact of a coccolithophore bloom on oceanic carbon uptake in the northeast Atlantic during summer 1991, Deep-Sea Res., 41, 297–314, 1994.
Roy, R. N., Roy, L. N., Vogel, R., Moore, C. P., Pearson, T., Good, C. E., Millero, F. J., and Campbell, D.: Determination of the ionization constants of carbonic acid in seawater, Mar. Chem., 44, 249–268, 1993.
Sabine, C. L., Key, R. M., Johnson, K. M., Millero, F. J., Poisson, A. P., Sarmiento, J. L., Wallace, D. W. R., and Winn, C. D.: Anthropogenic CO_2 inventory of the Indian Ocean, Global Biogeochem. Cy., 13, 179–198, 1999.
Sabine, C. L. and Feely, R. A.: Comparison of recent Indian Ocean anthropogenic CO_2 estimates with a historical approach, Global Biogeochem. Cy., 15, 31–42, 2001.
Salisbury, J. E., Green, M., Hunt, C., and Campbell, J.: Coastal acidification by rivers: A threat to shellfish? EOS, American Geophysical Union Transactions, 89(50), 513–528, 2008.
Semiletov, I., Makshatas, A. I., Akasofu, S.-I. and Andreas, E. L.: Atmospheric CO_2 balance: The role of arctic sea ice, Geophys. Res. Lett., 31(5), L05121, doi:10.1029/ 2003GL017996, 2004.
Serreze, M. C., Holland, M. M., and Stroeve, J.: Perspectives on the Arctic's shrinking sea-ice cover, Science, 315(5818), 1533–1536, doi:10.1126/science.1139426, 2007.
Springer, A. M., McRoy, C. P., and Flint, M. V.: The Bering Sea Green Belt: shelf-edge processes and ecosystem production, Fish. Oceanogr., 5, 205–223, 1996.
Stabeno, P. J., Bond, N. A., Kachel, N. B., Salo, S. A., and Schumacher, J. D.: On the temporal variability of the physical environment over the Southeastern Bering Sea, Fish. Oceanogr., 10, 81–98, 2001.
Stabeno, P. J., Kachel, N. B., Sullivan, M., Whitledge, T. E.: Variability of physical and chemical characteristics along the 70-m isobath of the Southeastern Bering Sea, Deep-Sea Res. Pt. II, 49, 5931–5943, 2002.

BGD
7, 7271–7314, 2010

Stockwell, D. A., Whitledge, T. E., Zeeman, S. I., Coyle, K. O., Napp, J. M., Brodeur, R. D., Pinchuk, A. I., and Hunt, G. L.: Anomalous conditions in the South-Eastern Bering Sea, 1997: nutrients, phytoplankton and zooplankton, Fish. Oceanogr. 10, 99–116, 2001.

Takahashi, T., Olafsson, J., Goddard, J. G., Chipman, D. W., and Sutherland, S. G.: Seasonal variation of CO_2 and nutrients in the high-latitude surface oceans: a comparative study, Global Biogeochem. Cy., 7(4), 843–878, 1993.

Takahashi, T., Sutherland, S. G., Sweeney, C., Poisson, A. P., Metzl, N., Tilbrook, B., Bates, N. R., Wanninkhof, R. H., Feely, R. A., Sabine, C. L., and Olafsson, J.: Biological and temperature effects on seasonal changes of pCO_2 in global ocean surface waters, Deep-Sea Res. Pt. II, 49, 1601–1622, 2002.

Takahashi, T., Sutherland, S. C., Wanninkhof, R., Sweeney, C., Feely, R. A., Chipman, D. W., Hales, B., Friederich, G. E., Chavez, F. P., Watson, A. J., Bakker, D. C. E., Schuster, U., Metzl, N., Yoshikawa-Inoue, H., Olafsson, J., Arnarson, T. S., Tilbrook, B., Johannessen, T., Olsen, A., Bellerby, R. J., Nojiri, Y., Wong, C. S., Delille, B., Bates, N. R., and de Baar, H. J. W.: Climatological mean and decadal change in surface ocean pCO_2, and net sea-air CO_2 flux over the global oceans, Deep-Sea Res. Pt. II, 56, 554–577, 2009.

Thomas, H., Schiettecatte, L.-S., Suykens, K., Koné, Y. J. M., Shadwick, E. H., Prowe, A. E. F., Bozec, Y., de Baar, H. J. W., and Borges, A. V.: Enhanced ocean carbon storage from anaerobic alkalinity generation in coastal sediments, Biogeosciences, 6, 267–274, doi:10.5194/bg-6-267-2009, 2009.

Walsh, J. J. and Dieterle, D. A.: CO_2 cycling in the coastal ocean. I – A numerical analysis of the Southeastern Bering Sea with applications to the Chukchi Sea and the Northern Gulf of Mexico, Progr. Oceanogr., 74, 335–392, 1994.

Walsh, J. J., Dieterle, D. A., Muller-Karger, F. E., Aagaard, K., Roach, A. T., Whitledge, T. E., and Stockwell, D.: CO_2 cycling in the coastal ocean. II. Seasonal organic loading of the Arctic Ocean from sources waters in the Bering Sea, Cont. Shelf Res., 17(1), 1–36, 1996.

Wanninkhof, R.: Relationship between wind speed and gas exchange over the ocean, J. Geophys. Res., 97, 7373–7382, 1992.

Weiss, R. F.: Carbon dioxide in water and seawater: the solubility of a non-ideal gas, Mar. Chem., 2, 203–215, 1974.

Wong, C. S., Waser, N. A. D., Nojiri, Y., Whitney, F. A., Page J. S., and Zeng, J.: Seasonal and interannual variability in the distribution of surface nutrients and dissolved inorganic carbon in the Northern North Pacific: influence of El Nino, J. Oceanogr., 58(2), 227–243, 2002.

BGD
7, 7271–7314, 2010

Wyllie-Echeverria, T. and Ohtani, K.: Seasonal sea ice variability and the Bering Sea ecosystem, in: Dynamics of the Bering Sea, edited by: Loughlin, T. and Ohtani, K., Univ. of Alaska Sea Grant Press, Fairbanks, Alaska, 435–451, 1999.

Zeebe, R. and Wolf-Gladrow, D.: CO_2 in Seawater: Equilibrium, Kinetics, Isotopes, Elsevier Oceanography Series 65, 2001.

Zondervan, I., Zeebe, R. E., Rost, B, and Riebesell, U.: Decreasing marine biogenic calcification: a negative feedback on rising atmospheric pCO_2, Global Biogeochem. Cy., 15, 507–516, 2001.

BGD

7, 7271–7314, 2010

Table 1. Estimates of the annual air-sea CO_2 flux on the Bering Sea shelf, assuming 500 000 km^2 of shelf area, and 180 days of open water.

Study	daily flux ($mmol\,CO_2\,m^{-2}\,d^{-1}$)	annual flux ($mol\,CO_2\,m^{-2}\,yr^{-1}$)	Bering Sea annual flux flux ($Tg\,C\,yr^{-1}$)
Walsh and Dieterle (1994)	n/a	4.3	3.4
Chen and Borges	−1.2[a] and 0.66[b]	n/a	11
Tahahashi et al. (2002)	2	n/a	37
This study	22 ± 3	n/a	157
Chen et al. (2004)	n/a	n/a	200

[a] Nedashkovskii and Sapozhnikov (2001),
[b] Codispoti et al. (1986)

BGD
7, 7271–7314, 2010

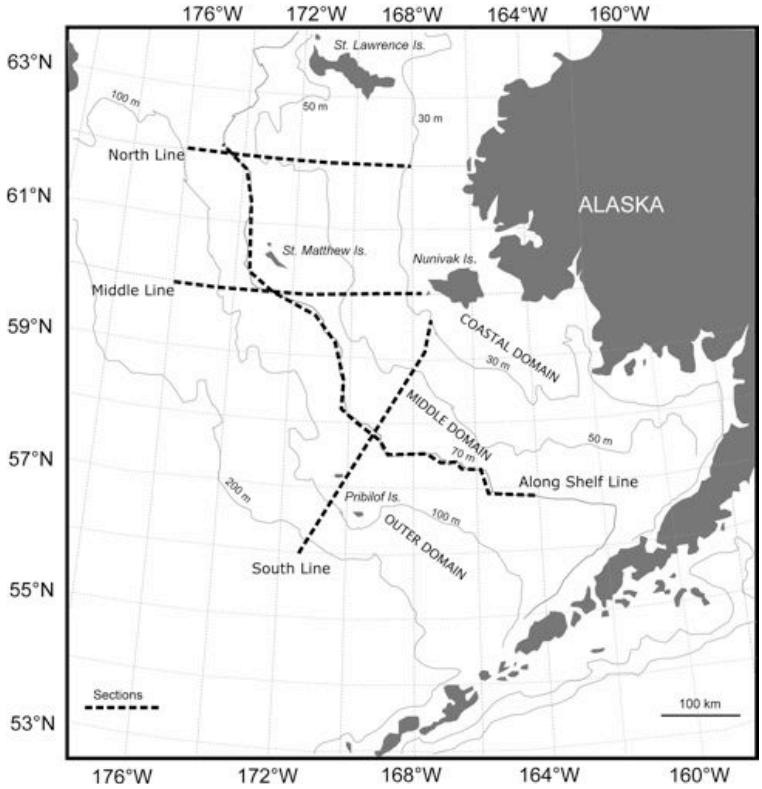

Fig. 1. Bering Sea shelf location map. The approximate positions of the North Line, Middle Line, South Line, and Along Shelf Line transects are shown on the figure. Approximate locations of the Coastal, Middle and Outer domains of the shelf are also shown.

BGD
7, 7271–7314, 2010

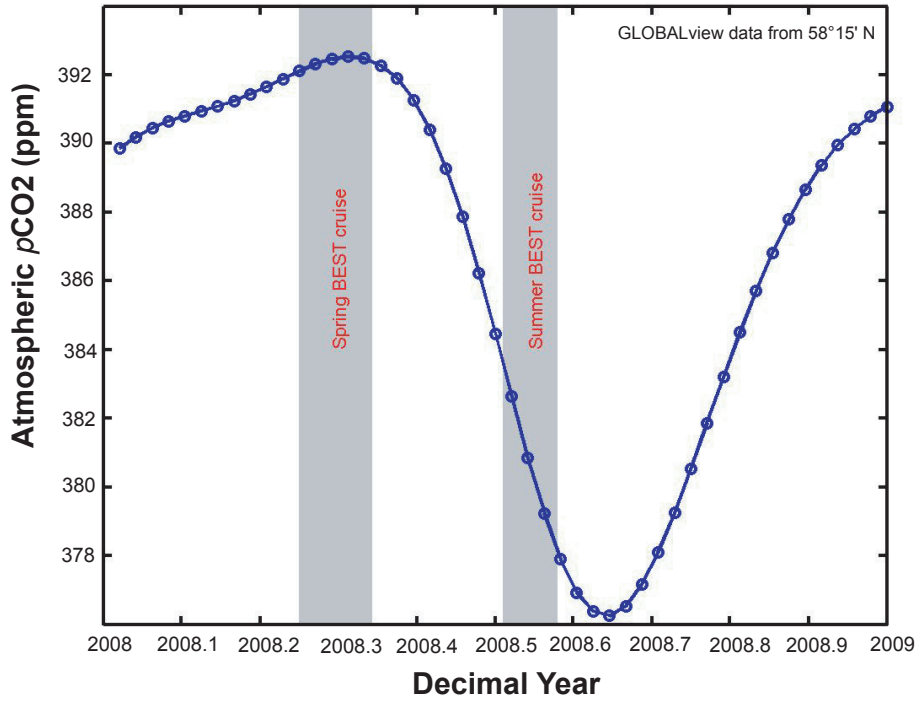

Fig. 2. Atmospheric CO_2 values (ppm) for the Bering Sea from GLOBALVIEW for 2008. The shaded areas represent the periods of time that the cruises were taking place. The atmospheric mixing ratio was then interpolated to the time each CTD hydrocast was conducted.

BGD
7, 7271–7314, 2010

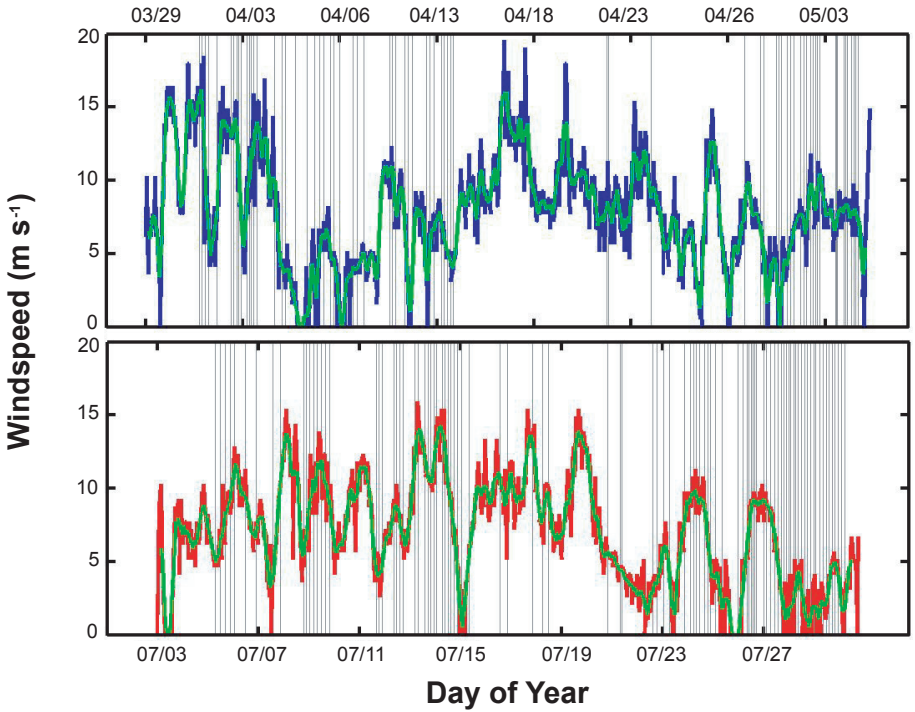

Fig. 3. Surface windspeed observations ($m\,s^{-1}$) from the USCGC Healy for both the spring (top plot) and summer (bottom plot) 2008 BEST cruises. In each plot, the original hourly wind data is shown in blue with the 6-h running mean shown in green. The grey lines indicate times of CTD casts.

BGD
7, 7271–7314, 2010

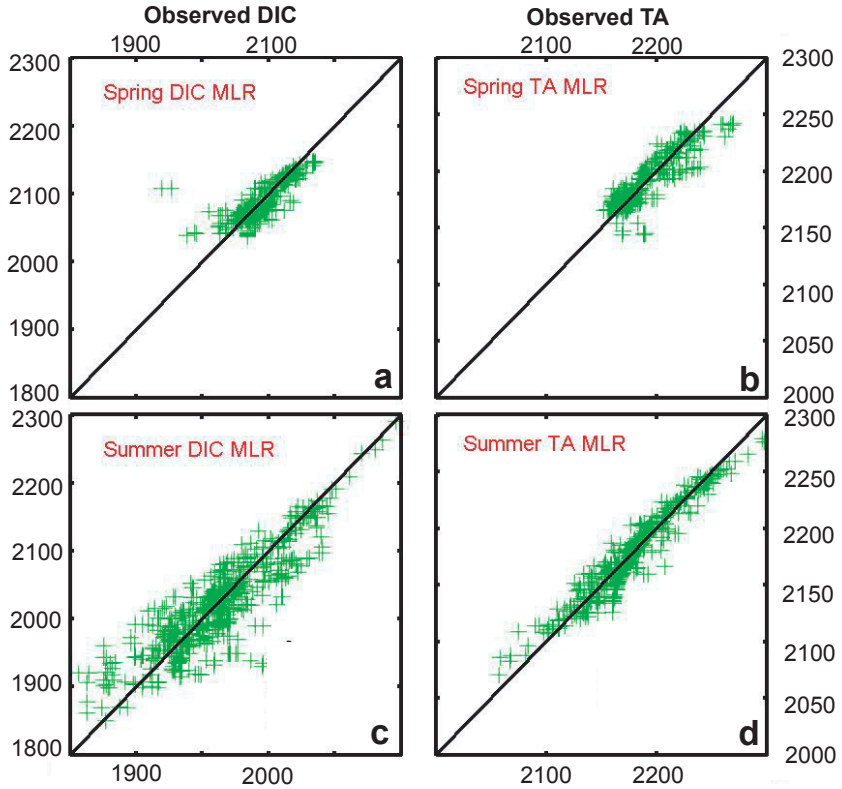

Fig. 4. **(a)** Interpolation of observed DIC using MLR approaches for the 2008 spring BEST cruise (std.dev 12.7 µmol kg^{-1}; r^2=0.63; n=368); **(b)** Interpolation of observed TA using MLR approaches for the 2008 spring BEST cruise (std.dev 8.4 µmol kg^{-1}; r^2=0.78; n=368); **(c)** Interpolation of observed DIC using MLR approaches for the 2008 summer BEST cruise (std.dev 27.9 µmol kg^{-1}; r^2=0.76; n=582); **(d)** Interpolation of observed TA using MLR approaches for the 2008 summer BEST cruise (std.dev 6.7 µmol kg^{-1}; r^2=0.92; n=582).

BGD
7, 7271–7314, 2010

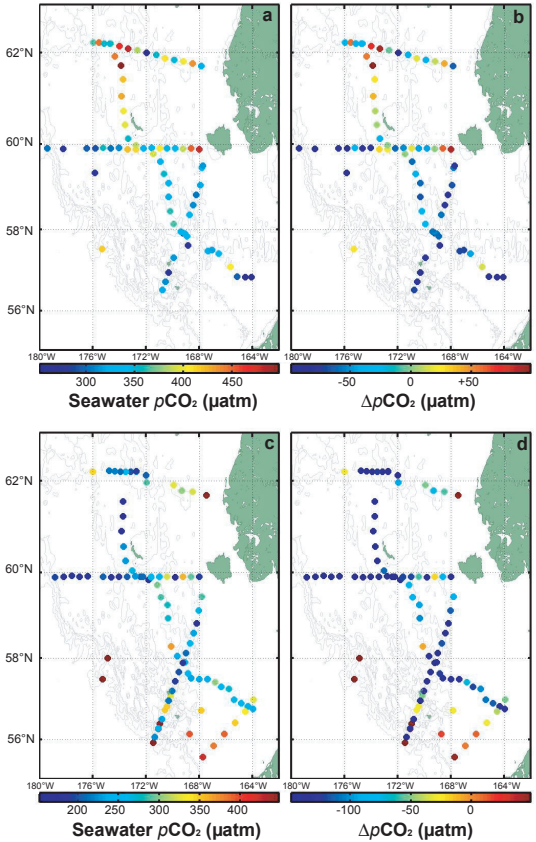

Fig. 5. Surface seawater pCO_2 and ΔpCO_2 values observed in spring and summertime during the 2008 BEST program. **(a)** Observed surface seawater pCO_2 at each hydrocast station during the 2008 spring BEST cruise; **(b)** Observed seawater ΔpCO_2 at each hydrocast station during the 2008 spring BEST cruise; **(c)** Observed seawater pCO_2 at each hydrocast station during the 2008 summer BEST cruise; **(d)** Observed seawater ΔpCO_2 at each hydrocast station during the 2008 summer BEST cruise.

BGD
7, 7271–7314, 2010

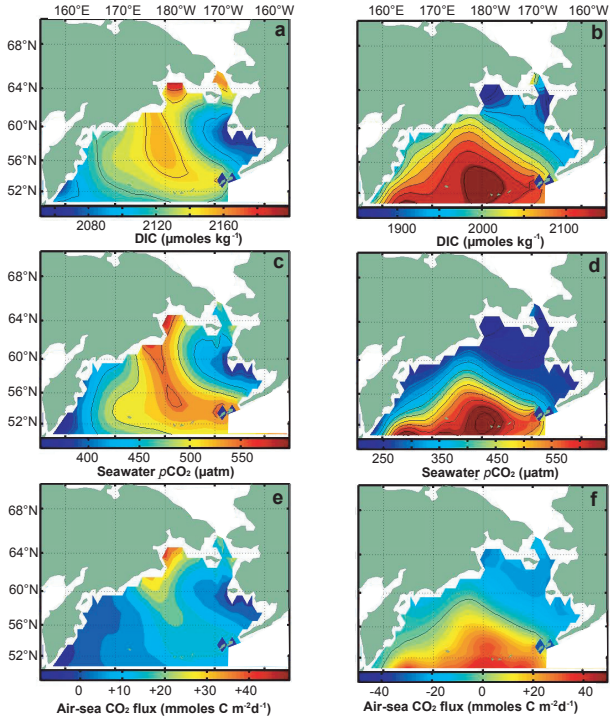

Fig. 6. Surface climatological maps of seawater carbonate properties and air-sea CO_2 flux determined using the MLR-based model. **(a)** springtime DIC ($\mu mol\,kg^{-1}$); **(b)** summertime DIC ($\mu mol\,kg^{-1}$); **(c)** springtime seawater pCO_2 (μatm); **(d)** summer seawater pCO_2 (μatm); **(e)** springtime air-sea CO_2 flux ($mmol\,m^{-2}\,d^{-1}$); **(f)** summertime air-sea CO_2 flux ($mmol\,m^{-2}\,d^{-1}$).

BGD
7, 7271–7314, 2010

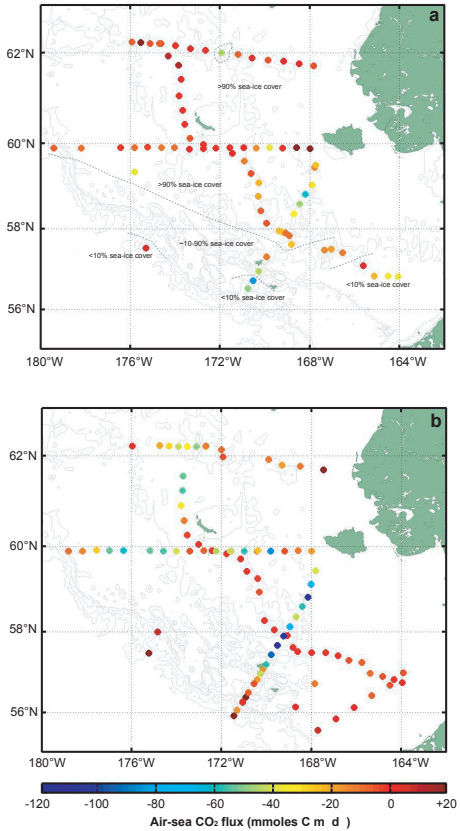

Fig. 7. Air-sea CO_2 flux values calculated at each CTD/hydrocast station in spring and summetime during the 2008 BEST program. **(a)** Estimated air-sea CO_2 flux (mmol CO_2 m^{-2} d^{-1}) at each hydrocast station during the 2008 spring BEST cruise; **(b)** Estimated air-sea CO_2 flux (mmol CO_2 m^{-2} d^{-1}) at each hydrocast station during the 2008 summer BEST cruise.

BGD
7, 7271–7314, 2010

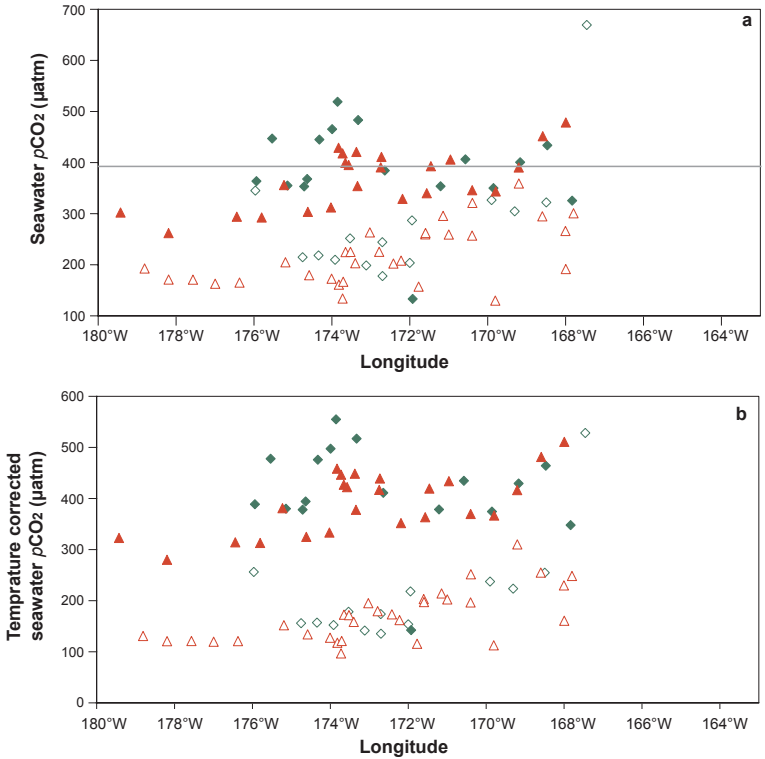

Fig. 8. Surface seawater pCO_2 (panel **a**) and temperature corrected seawater pCO_2 (panel **b**) plotted against longitude for the Northern Bering Sea shelf at the North Line (red symbols) and Middle Line (green symbols). Temperature corrected seawater pCO_2 was based on corrected to 0 °C using the empirical relationships of Takahashi et al., 2002. Spring and summer data was shown with closed and open symbols, respectively. In the panels, the nearshore to offshore transition is shown from right to left (i.e., east to west).

BGD
7, 7271–7314, 2010

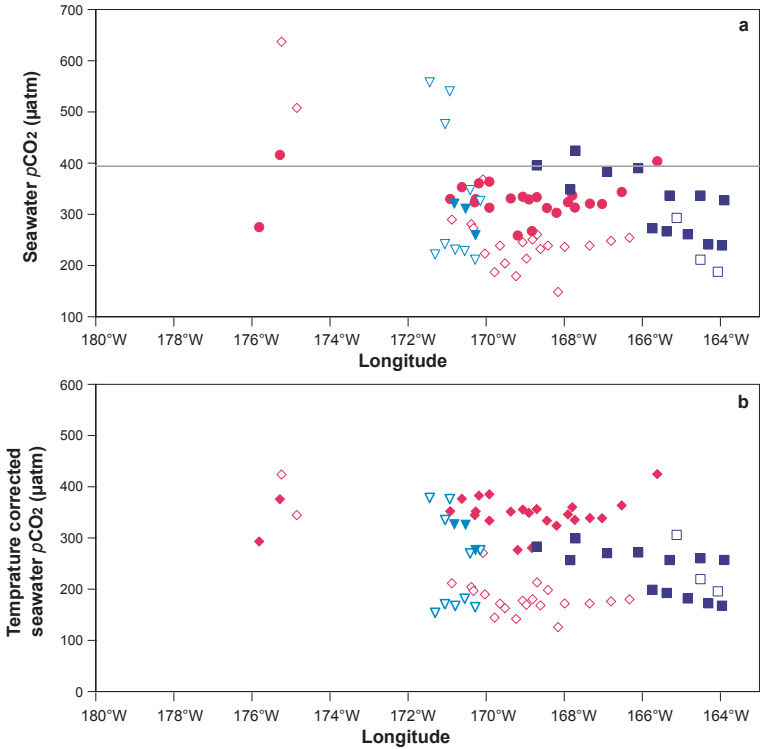

Fig. 9. Surface seawater pCO_2 (µatm; panel **a**) and temperature corrected seawater pCO_2 (µatm; panel **b**) plotted against longitude for the Southern Bering Sea shelf for the following regions: (1) between Nunavak Island and Pribilof Islands (pink symbols); (2) south of Pribilof Islands (blue symbols), and; (3) SE Bering Sea shelf (turquoise symbols). Temperature corrected seawater pCO_2 was based on corrected to 0 °C using the empirical relationships of Takahashi et al. (2002). Spring and summer data was shown with closed and open symbols, respectively. In the panels, the nearshore to offshore transition is shown from right to left (i.e., east to west).

BGD
7, 7271–7314, 2010

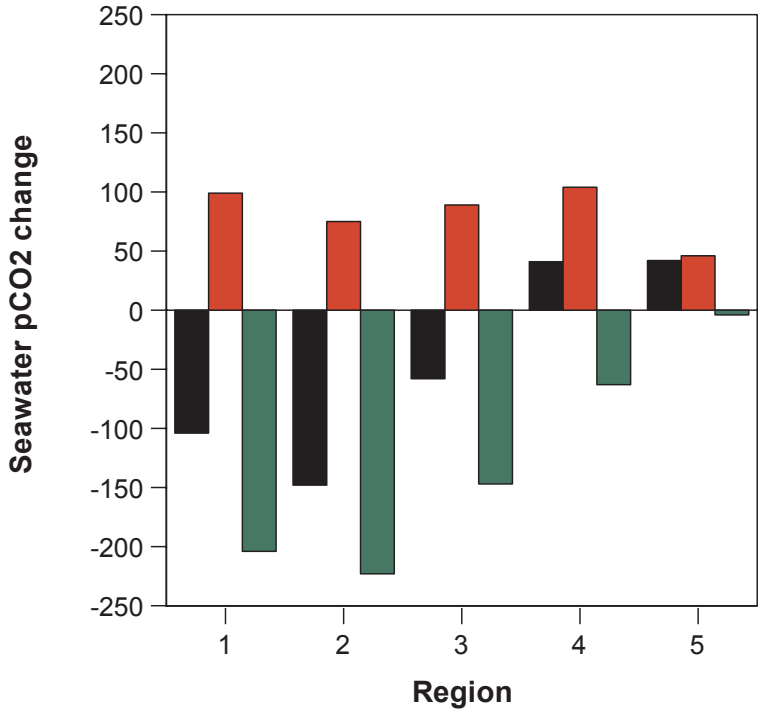

Fig. 10. Temperature and the "net biology" effects on seasonal change in observed seawater pCO_2 (µatm) for the following regions of the Bering Sea shelf: (1) the North Line; (2) the Middle Line; (3) between Nunavak Island and Pribilof Islands, (4) south of the Probilof Islands, and; (5) SE Bering Sea shelf. In the bar chart, the black column denotes the mean observed change in seawater pCO_2 for each region (i.e., $\delta pCO_2^{\text{spring-summer}}$ in Eq. 7), while the red and green columns indicates the changes imparted by temperature ($\delta pCO_2^{\text{temperature}}$) and "net biology" ($\delta pCO_2^{\text{biology}}$), respectively.

BGD
7, 7271–7314, 2010

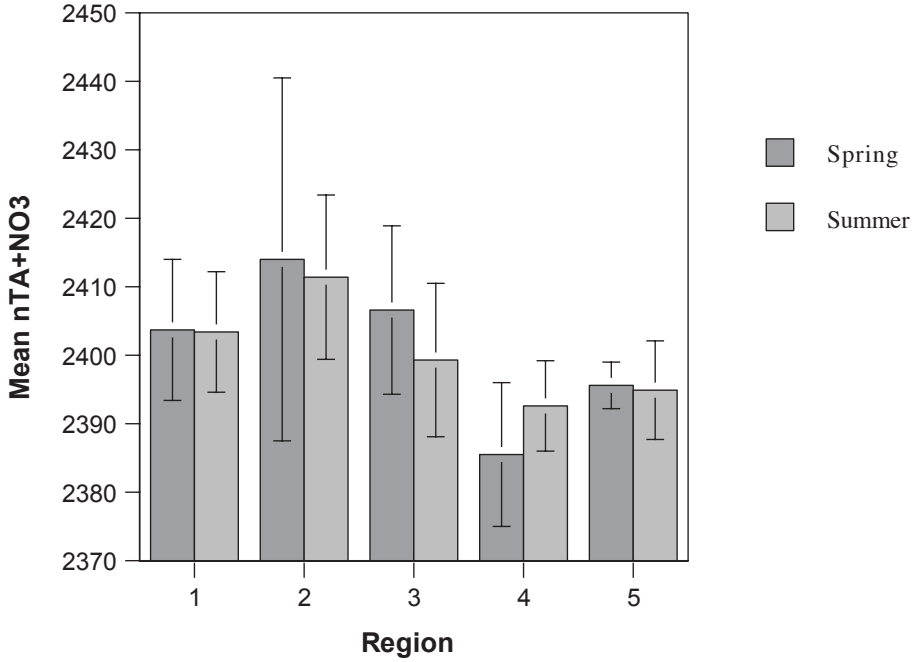

Fig. 11. Spring to summer changes in observed surface nTA+NO_3 (μmol kg^{-1}) for the following regions of the Bering Sea shelf: (1) the North Line; (2) the Middle Line; (3) between Nunavak Island and Pribilof Islands, (4) south of the Probilof Islands, and; (5) SE Bering Sea shelf.

BGD
7, 7271–7314, 2010

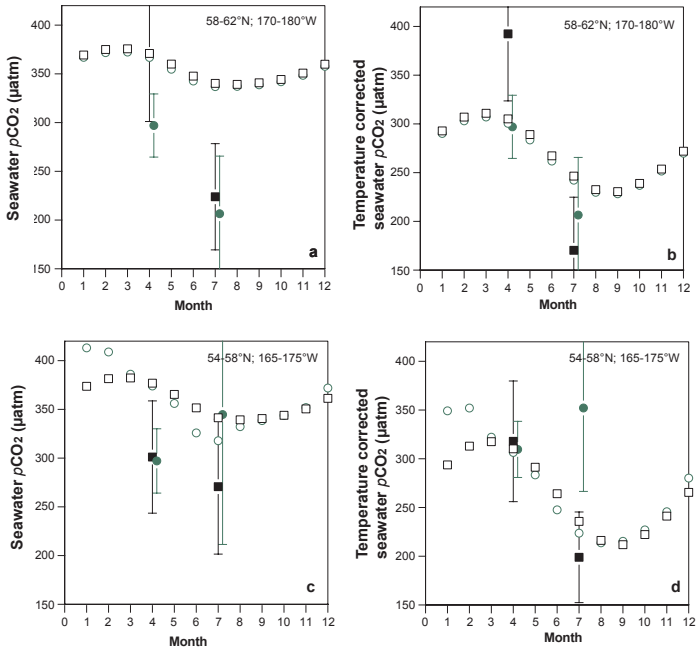

Fig. 12. Comparison of Takahashi et al. (2009) surface seawater pCO_2 and temperature corrected seawater pCO_2 climatology for the Bering Sea shelf with observations from the 2008 BEST spring and summer cruises. The Takahashi et al. (2009) data have a spatial resolution of 4°×5° and monthly resolution. 2008 BEST spring and summer are binned and averaged within each of four Takahashi et al. (2009) 4°×5° that are defined for the Bering Sea shelf. Please note that the mean values for observed data from the two 4°×5° areas have been slightly offset in time to allow for easier interpretation of data. **(a)** surface seawater pCO_2 for the 58° N–62° N/170° W–175° W (black symbols), and 58° N–62° N/175° W–180° W (green symbols) areas. In each of the panels, Tahahashi et al. (2009) climatology data are shown by open symbols while 2008 BEST spring and summer are shown as closed symbols (mean and 1 std deviation); **(b)** surface temperature corrected seawater pCO_2 for the 58° N–62° N/170° W–175° W (black symbols), and 58° N–62° N/175° W–180° W (green symbols) areas; **(c)** surface seawater pCO_2 for the 54° N–58° N/165° W–170° W (black symbols), and 54° N–58° N/170° W–175° W (green symbols) areas; and; **(d)** surface temperature corrected seawater pCO_2 for the 54° N–58° N/165° W–170° W (black symbols), and 54° N–58° N/170° W–175° W (green symbols) areas. For the temperature corrected seawater pCO_2 datasets, both Takahashi et al. (2009) and 2008 BEST spring and summer data were corrected to 0 °C using the empirical relationships of Takahashi et al. (2002).

BGD
7, 7271–7314, 2010